

# Numerical Analysis of the Hydrodynamics of Proximity Impellers using the SPH Method

Maria Soledad Hernández-Rivera<sup>a</sup>, Karen Guadalupe Medina-Elizarraraz<sup>a</sup>, Jazmín Cortez-González<sup>a,\*</sup>, Rodolfo Murrieta-Dueñas<sup>a</sup>, Carlos E. Alvarado-Rodríguez<sup>b,c</sup>, José de Jesús Ramírez-Minguela<sup>b</sup>, Juan Gabriel Segovia Hernández<sup>b</sup>

<sup>a</sup> Tecnológico Nacional de México / Campus Irapuato, Departamento de Ingeniería Química, Irapuato, Guanajuato, México

<sup>b</sup> Universidad de Guanajuato, Departamento de Ingeniería Química, Guanajuato, Guanajuato, México.

<sup>c</sup> Secretaría de Ciencias, Humanidades, Tecnología e Innovación, Ciudad de México, México

\* Corresponding Author: [jazmin.cg@irapuato.tecnm.mx](mailto:jazmin.cg@irapuato.tecnm.mx)

## ABSTRACT

Mixing is a critical operation in numerous industrial processes, traditionally performed in agitated tanks to ensure homogenization. Despite its importance, the design of tanks and impellers is often neglected during agitation system selection, resulting in excessive energy consumption and inefficient mixing. To mitigate these challenges, Computational Fluid Dynamics (CFD) serves as a powerful tool for analyzing tank hydrodynamics and quantifying mixing times. CFD employs mathematical models to simulate mass, heat, and momentum transport phenomena within fluid systems. Among the latest advancements in modeling stirred tank hydrodynamics is Smoothed Particle Hydrodynamics (SPH), a mesh-free Lagrangian approach that tracks individual particles characterized by properties such as mass, position, velocity, and pressure. SPH provides significant advantages over traditional mesh-based methods by accurately capturing fluid behavior through particle interactions. In this study, the performance of three impellers—double ribbon, paravisc, and hybrid—was evaluated based on hydrodynamics and mixing times during the homogenization of water and ethanol in a 0.5 L stirred tank. The tank and impellers were meticulously designed, operating at 70% capacity, with the fluids exhibiting the following rheological properties:  $\rho_1 = 1000 \text{ kg/m}^3$ ,  $\rho_2 = 789 \text{ kg/m}^3$ ,  $\mu_1 = 1\text{E-}6 \text{ m}^2/\text{s}$ , and  $\mu_2 = 1.52\text{E-}6 \text{ m}^2/\text{s}$ . The simulations were conducted under turbulent flow conditions (Reynolds number of 10,000) for a duration of 2 minutes using the DualSPHysics software. The stirring speed was set at 34 rpm, and the initial particle spacing was configured to 1 mm, generating 270,232 fluid particles and 187,512 boundary particles representing the tank and agitator. The analysis included velocity profiles, flow patterns, vorticity, divergence, and density fields to assess mixing performance. The Q-criterion was employed to discern the dominance of rotational or deformational motion and to identify stagnation zones. The results revealed that the double ribbon impeller exhibited superior performance, achieving 88.28% mixing within approximately 100 seconds, while the paravisc and hybrid impellers reached mixing efficiencies of 12.36% and 11.8%, respectively. These findings underscore the potential of SPH as a robust computational approach for linking hydrodynamic behavior with mixing efficiency and identifying key parameters to optimize mixing processes.

**Keywords:** CFD, hydrodynamics, Proximity impellers, SPH, homogenization

## 1. INTRODUCTION

The numerical analysis of fluid distribution in stirred tanks is an essential tool for evaluating impeller performance. It enables the characterization of axial and radial

flow patterns, velocity profiles, mixing times, stagnation zones, and vortex formation. These analyses are typically conducted using Computational Fluid Dynamics (CFD), which provides detailed insights that are often unattainable through experimental methods. However, CFD

simulations demand significant computational resources (Gelves et al., 2013). Analyzing mixing times numerically is particularly valuable for understanding the distribution of species within chemical or biological reactors. This parameter is critical for assessing the overall effectiveness of stirred tanks. Previous studies have extensively investigated the influence of stirrer geometry on hydrodynamics and mixing times in such reactors. Many of these efforts have focused on optimizing conventional impellers, such as the Rushton turbine, to enhance their performance. Despite these advances, there has been limited investigation into proximity impellers—specialized designs that operate at a short distance from the tank walls. These impellers are commonly employed for mixing non-Newtonian fluids and are characterized by lower operational speeds compared to conventional designs. In this work, the mixing process for achieving a homogeneous 50% water-ethanol solution is simulated using the Smoothed Particle Hydrodynamics (SPH) method. The primary objective is to develop a robust methodology for analyzing the hydrodynamics of mixing processes in stirred tanks equipped with different impeller designs. The performance of the impellers is subsequently compared to identify the most effective option for the fluids under investigation.

## 2. METHODOLOGY

### 2.1 CAD design of the impellers

In this work, three proximity impellers: double ribbon, paravisc and hybrid, were used to simulate the mixing process of the ethanol-water solution. Figure 1 shows the proximity impellers analyzed. The double Ribbon agitator consists of two opposite helical ribbons fitted on an axis, one of these ribbons has the job of moving the materials to be mixed in a single direction and the other does the same as the previous one, however, it does it in an opposite direction, as a consequence of these movements the materials to be mixed acquire a single direction, making this system ideal to be used as a continuous mixer (Londoño, 2019). This impeller is generally used in industries to be able to combine powdered, granulated and viscous materials. The effectiveness of the mixing process will depend on factors, such as the rotation speed, the design of the belts, the mixing time and the physical properties of the materials (Flores & Cuevas, 2008).

Paravisc is a proximity impeller that works efficiently with high viscosity mixtures, however, it can be coupled to different stages of the process with the possibility of accomplishing an efficient homogenization. This type of impeller, like the previous one, works inside a mixing tank with circular geometry, in which there is a minimum separation with the internal wall of the tank and also the space between the blades and the bottom surface, which

means that the mechanical operation of this impeller is made circular through the action of the axial pumping. This type of impeller can work without problem with internal baffles to improve power, heat transfer and to obtain an adequate mixing incorporating all the solids of the more viscous medium. The hybrid agitator is a novel design reported by Alvarado-Rodríguez et al. (2023). It is a proximity stirrer that combines the characteristics of the anchor stirrer with the double ribbon stirrer. Its efficiency lies in favoring mixing in both axial and radial directions.

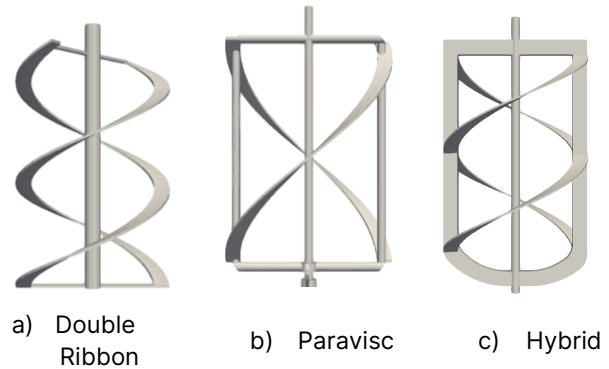


**Figure 1.** CAD design of the selected proximity impellers.

### 2.2 SPH method

Computational Fluid Dynamics (CFD) simulation has proven to be a powerful tool to study and optimize mixing processes, contributing to the development of more efficient processes (Yin, et al., 2022). CFD numerical analysis allows a better comprehension of the momentum, mass and energy transport phenomena of different systems. In stirring systems, emulsification, homogenization and mixing mechanisms are analyzed numerically to describe the behavior of fluids inside the tank (Zawawi, et al., 2018).

Recently, within computational fluid dynamics, the method of smoothed particle hydrodynamics has been implemented to analyze the behavior of fluids. SPH is a method for meshless Lagrangian and dissipative particle dynamics transporting physical properties such as mass, position, velocity and pressure. It is able to follow the trajectory of these particles, can analyze highly complex flows and where there are deformations or phenomena at macro or meso scale. It is able to handle complex geometries and boundary conditions. SPH tracks individual fluid particles by calculating their interactions to simulate the fluid behavior. Equations 1 to 3 present the equations describing the hydrodynamics of stirred tanks.

$$\frac{d\rho}{dt} = -\rho \nabla \cdot \mathbf{v}, \quad (1)$$

$$\frac{d\mathbf{v}}{dt} = -\frac{\nabla P}{\rho} + \frac{\mu}{\rho} \nabla^2 \mathbf{v} + \mathbf{g}, \quad (2)$$

$$\frac{dC}{dt} = D\nabla^2 C - \nabla \cdot (C\mathbf{v}) + \mathbf{v} \cdot \nabla C, \quad (3)$$

where:  $\rho$  is the density,  $t$  is time,  $\mathbf{v}$  is velocity,  $P$  is pressure,  $\mu$  is viscosity,  $\mathbf{g}$  is gravity,  $C$  is concentration and  $D$  is the mass diffusion coefficient.

Equations 1 to 3 are shown in the SPH formalism in equations 4 to 6 which are closed by the Tait's equation of state shown in the equation 7

$$\frac{d\rho_a}{dt} = -\rho_a \sum_b^n m_b \frac{\mathbf{v}_b}{\rho_b} \cdot \nabla W_{ab} \quad (4)$$

$$\begin{aligned} \frac{d\mathbf{v}_a}{dt} = & - \sum_b^n m_b \left( \frac{p_a + p_b}{\rho_a \rho_b} \right) \nabla_a W_{ab} \\ & + 2\nu \sum_b^n m_b \frac{\mathbf{v}_{ab} r_{ab} \cdot \nabla W_{ab}}{\bar{\rho}_{ab} r_{ab}^2 + \varepsilon^2} + \mathbf{g} \end{aligned} \quad (5)$$

$$\begin{aligned} \frac{dC_a}{dt} = & \sum_b^n m_b \frac{C_{ab} D \cdot \nabla W_{ab}}{\rho_b r_{ab}^2 + \varepsilon^2} \\ & - \sum_b^n m_b \frac{C_b}{\rho_b} (\mathbf{v}_a \cdot \nabla_a W_{ab}) \end{aligned} \quad (6)$$

$$p = B \left[ \left( \frac{\rho}{\bar{\rho}} \right)^\gamma - 1 \right] \quad (7)$$

where the subscripts  $a, b$  are referent to the mean particle  $a$  or neighbor particles  $b$ ,  $W$  is the kernel function,  $m$  is the mass of the particle,  $r_{ab} = r_a - r_b$ , where  $r$  is the position vector,  $\nu$  is the kinematic viscosity,  $\bar{\rho}_{ab} = \frac{\rho_a + \rho_b}{2}$ ,  $D$  is the diffusion coefficient,  $C_{ab} = C_a - C_b$ ,  $\varepsilon$  is a small regularization term to prevent singularities,  $B = c^2 \rho / \gamma$ ,  $\gamma = 7$  for liquids,  $\bar{\rho}$  is a reference density and  $c$  is a numerical speed of sound which must be at least 10 times higher than the maximum velocity of the fluid in the system to ensure a maximum density fluctuation of 1% satisfying the compressibility condition.

Finally, the properties of the particles as de density, position, velocity and concentration are advanced from time  $t^{n+1} = t^n + \Delta t$  using the Verlet algorithm according to equations 8 to 11.

$$\rho_a^{n+1} = \rho_a^{n-1} + 2\Delta t \left( \frac{d\rho_a}{dt} \right)^n, \quad (8)$$

$$\mathbf{r}_a^{n+1} = \mathbf{r}_a^n + \Delta t \mathbf{v}_a^n + 0.5\Delta t^2 \left( \frac{d\mathbf{x}_a}{dt} \right)^n, \quad (9)$$

$$\mathbf{v}_a^{n+1} = \mathbf{v}_a^{n-1} + 2\Delta t \left( \frac{d\mathbf{v}_a}{dt} \right)^n, \quad (10)$$

$$C_a^{n+1} = C_a^{n-1} + 2\Delta t \left( \frac{dC_a}{dt} \right)^n, \quad (11)$$

Where  $n$  is the value of step and  $\Delta t$  is the time step calculated with the equation 12.

$$\Delta t = \min \left[ \left( \frac{h}{d\mathbf{v}_a/dt} \right)^{1/2}, \frac{h}{(c + \Delta t_{v,a})}, \frac{h^2}{2D} \right] \quad (12)$$

Where  $h$  is the smoothing length of the kernel function and  $\Delta t_{v,a} = \max_b |h r_{ab} \cdot \mathbf{v}_{ab} / (r_{ab} \cdot r_{ba} + \varepsilon^2)|$ .

Using the Verlet algorithm, numerical coupling of the discrete SPH equations is ensured during the evolution by alternating the step  $t^{n-1}$  in in the first term of the right side in equations 8, 10 and 11 every  $N \approx 40$  steps by the step  $t^n$ .

### 2.3 Numerical simulation

Numerical simulations were performed using the DualSPHysics software (Domínguez et al., 2022) which is based on the SPH method. The tank and impellers geometries generated in CAD were imported into the DualSPHysics software to generate the fixed and moving boundary conditions in the simulation. The tank was filled to 70% volume, being 35% water at the bottom and 35% ethanol at the top of the liquid. An isothermal mixing process at 25°C was considered. The initial distance between particles is 1 mm generating a total of 270232 fluid particles and 187512 contour particles (tank plus stirrer). The initial velocity of the liquids is zero and a no-slip boundary condition is established on the tank surface. The stirring speed for the three stirrers is 33.9 rpm setting a Reynolds number of 10000. The initial stirrer speed is zero and is accelerated at 16.95 rpm for 1 second until the constant stirring speed is reached. Two minutes of mixing time was simulated and the percentage of mixing over time was evaluated, as well as the average velocity after 1.5 minutes of stirring. The fluid parameters used in the simulation are shown in Table 1.

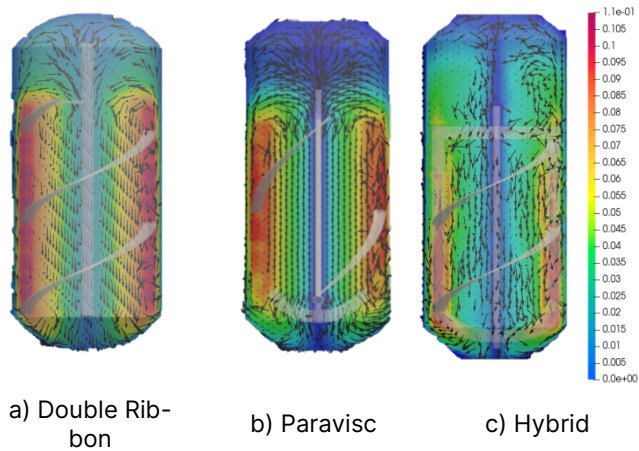
**Table 1.** Properties of water, ethanol and the mixture.

	Water	Ethanol	Mixture
Density (kg/m <sup>3</sup> )	1000	789	894.5
Kinematic Viscosity (m <sup>2</sup> /s)	1 E-06	1.52 E -06	1.17 E-06

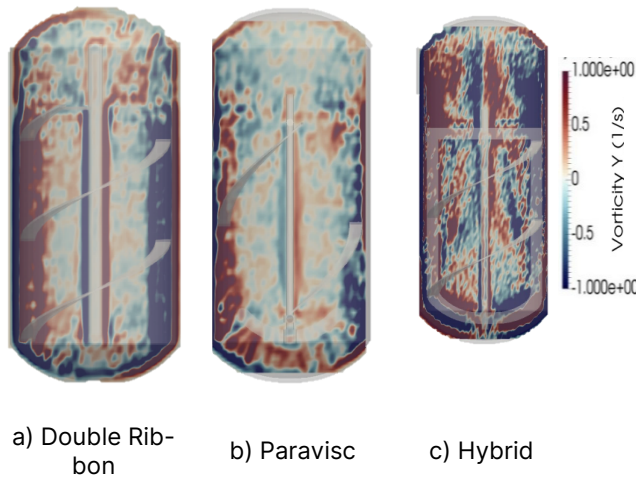
## 4. RESULTS

The numerical simulations provided detailed insights into the mixing performance and hydrodynamic behavior within the stirred tank. Key parameters such as the mixing percentage over the simulated time, average velocity, velocity gradient, divergence, and vorticity of the flow were quantified. Additionally, the Q-criterion was employed to further analyze the hydrodynamic characteristics of the fluid within the tank. Density and density gradient fields within the tank were also visualized to identify regions of high mixing efficiency and to evaluate the relationship between the mixing performance and the flow patterns generated by each impeller. The primary

goal was to determine which impeller achieved the highest mixing percentage within 2 minutes and to correlate this performance with the hydrodynamic features induced by the impeller design. Figure 2 illustrates the average velocity profiles for the different impellers. For all configurations, the highest velocity was observed near the tank walls. Furthermore, vortices were consistently present in the regions of highest velocity for each impeller. These vortices facilitated fluid circulation, directing the flow upward along the tank walls and creating a downward flow in the central region of the tank. This circulation pattern played a crucial role in promoting effective mixing within the tank.



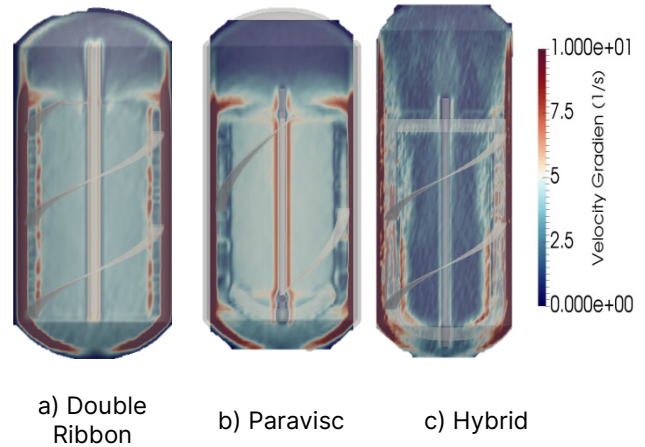
**Figure 2.** Average velocity generated by the impellers inside the tank.



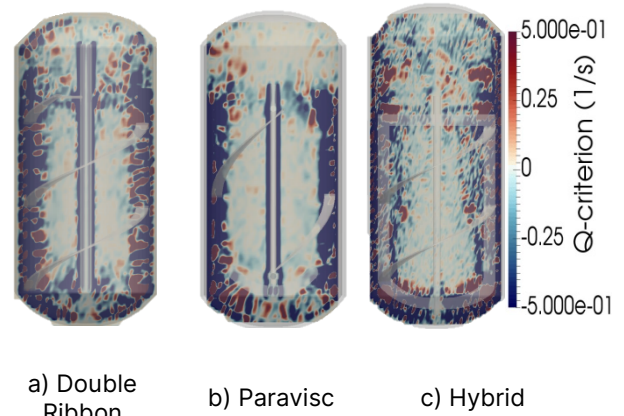
**Figure 3.** Vorticity calculated from the average velocity.

Figure 3 shows the behavior of the vorticity generated by the fluid inside the tank in each impeller. The red color represents regions of high vorticity, indicating strong twists and rotations of the fluid in those areas. These regions usually form near the proximity stirrer blades due to the force imposed on the fluid. Conversely,

low vorticity zones (blue color), indicate areas of more stable and less disturbed flow, suggesting a limited mixing pattern in this region. The intermediate colors show a more efficient and homogeneous mixing. Figure 4 shows the velocity gradient of the fluid inside the tank. This value indicates the change of direction of the fluid with respect to the movement of the impeller. According to Figure 4, the gradient is higher near the wall. However, the zone with the lowest gradient, which is the center, represents only half of this gradient.



**Figure 4.** Velocity gradient inside the tank.



**Figure 5.** Criterion Q obtained inside the tank.

Figure 5 is presenting the Q Criterion in our system which gives us a trend for zones where rotation is dominant over deformation. For positive values of Q the rotation is dominant and for negative values of Q the deformation is dominant. According to the results obtained, in the paravisc and hybrid proximity impellers shakers the fluid deformation predominates over vorticity, that is, the divergence value is much higher than the vorticity value mainly in the proximity of the impeller, this suggests that this type of impellers is recommended for viscous fluids or non-Newtonian fluids. Figure 6 shows the density field with the different impellers over time from 0 to 60

seconds, which is related to the mixing inside the tank. Initially, water is at the bottom and ethanol at the top. The volume fraction of both components corresponds to 50%. With the double ribbon impeller, a density field with values close to the density of the mixture is generated after 36 seconds and increases considerably after 60 seconds. For the paravisc impeller, the evolution of the density change is obtained in a representative manner up to 60 seconds of mixing. Using the paravisc impeller, it is observed that the mixing is obtained mainly in the center of the tank. Finally, the Hybrid impeller presents an intermediate homogenization between the paravisc impeller and the double ribbon impeller.

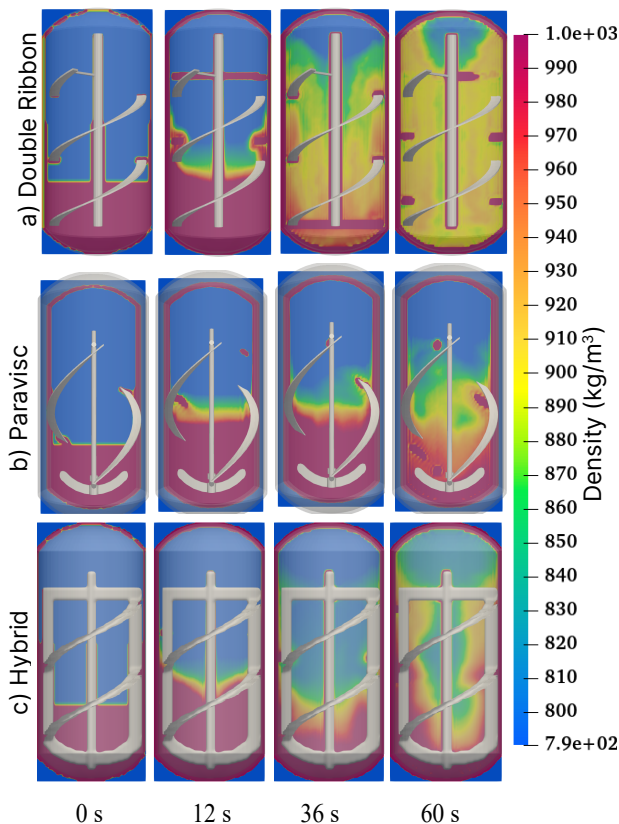


**Figure 6.** Density field at different times obtained in all cases.

## 5. CONCLUSIONS

This study presents a numerical analysis of the hydrodynamics of different impellers to evaluate their performance based on velocity profiles, vorticity, divergence, and the Q-criterion, which correlates fluid deformation with rotational motion within a stirred tank. The results demonstrate that the Double Ribbon impeller exhibited significantly superior performance compared to the Paravisc and hybrid impellers, achieving a mixing

efficiency of 88.28% within approximately 100 seconds. The exceptional performance of the Double Ribbon impeller can be attributed to its unique design, featuring two intertwined ribbons that promote a more uniform and turbulent flow within the tank. This design enhances mixing efficiency and ensures effective homogenization of the fluid mixture. The findings underscore the critical role of impeller design in optimizing mixing performance and highlight the Double Ribbon impeller as a highly effective solution for applications requiring efficient and rapid homogenization.

## ACKNOWLEDGEMENTS

We are in agreement with the National Technological Institute of Mexico for the support provided for this research. C.E.A.R thanks SECIHTI for the support provided through project 368 within the program Investigadoras e Invetsigadores por México.

## REFERENCES

1. Chambergó, J.C., Valverde, Q., Pachas, A. A., & Yepez, H. (2017). Estudio del Comportamiento Fluido-Dinámico de un Agitador a Escala Reducida Mediante Simulación Numérica. *Información tecnológica*, vol. 28(3), 37-46.
2. Flores, C. J., & Cuevas, C. N. (2008). Diseño de una mezcladora dosificadora de cremas cosméticas. [Tesis de licenciatura, Escuela Politécnica Nacional]. Repositorio Digital - EPN.
3. Gil, I. D., Guevara, J. R., García, J. L., Leguizamón, A., & Rodríguez, G. (2016). *Process Analysis and Simulation in Chemical Engineering*. Springer International Publishing.
4. Londoño, J. (2019). Propuesta de mejora en la línea de vegetales para la empresa PANAMERICANA DE ALIMENTOS SAS, mediante un sistema automático de transporte dosificación y mezcla de granos. [Tesis de licenciatura, INSTITUTO TECNOLÓGICO METROPOLITANO]. Repositorio Institucional ITM.
5. Miño Valdés, J. E., Benítez Cortés, I., & Pérez Martínez, A. (2020). Simulación de procesos químicos y aplicaciones del simulador SuperPro Designer. Universidad Nacional de Misiones.
6. Monaghan, J. J. (1992). Smoothed Particle Hydrodynamics, *Annual Review of Astronomy and Astrophysics*, Volume 30, 543-574,
7. Rodríguez, J.C., Luviano, J.L. & Vargas, J.C. (2018). Análisis de la hidrodinámica de fluidos en tanques agitados. *JOVENES DE LA CIENCIA Revista de Divulgación Científica*, Vol. 4 (no. 1), 5(2), 3036.
8. Uribe, A. R., Rivera, R., Aguilera, A., y Murrieta, E. (2012). *AGITACION Y MEZCLADO*. Departamento de Ingeniería Química, División de Ciencias

Naturales y Exactas, Universidad de Guanajuato.  
Repositorio Institucional de la Universidad de  
Guanajuato.

[http://repositorio.ugto.mx/bitstream/20.500.12059/6256/1/3\\_Agitaci%c3%b3n%20y%20mezclado.pdf](http://repositorio.ugto.mx/bitstream/20.500.12059/6256/1/3_Agitaci%c3%b3n%20y%20mezclado.pdf)

9. Ye, T., Pan, D., Huang, C., & Liu, M. (2019). Smoothed particle hydrodynamics (SPH) for complex fluid flows: Recent developments in methodology and applications. *Physics of Fluids*, 31(1).
  10. Yin, C., Zheng, K., He, J., Xiong, Y., Tian, Z., Lin, Y., & Long, D. (2022). Turbulent CFD Simulation of Two Rotor-Stator Agitators for High Homogeneity and Liquid Level Stability in Stirred Tank. *Materials*, 15(23), 8563. <https://doi.org/10.3390/ma15238563>
- Zawawi, M. H., Saleha, A., Salwa, A., Hassan, N. H., Zahari, N. M., Ramli, M. Z., & Muda, Z. C. (2018). A review: Fundamentals of computational fluid dynamics (CFD). In *AIP conference proceedings*, vol. 2030, No. 1.

---

© 2025 by the authors. Licensed to PSEcommunity.org and PSE Press. This is an open access article under the creative commons CC-BY-SA licensing terms. Credit must be given to creator and adaptations must be shared under the same terms. See <https://creativecommons.org/licenses/by-sa/4.0/>

